CONF-760935 - P 4

Proceedings of the Second Topical Meeting on

The Technology of Controlled Nuclear Fusion

Volume IV

September 21-23, 1976 Richland, Washington

Sponsored by

Richland Section and Controlled Nuclear Fusion Division of American Nuclear Society
Electric Power Research Institute
and U.S. Energy Research and Development Administration

U.S. ENERGY RESEARCH AND DEVELOPMENT ADMINISTRATION

TOKAMAK EXPERIMENTAL POWER REACTOR PRIMARY ENERGY CONVERSION SYSTEM *

H. C. Stevens, M. A. Abdou, R. F. Mattas, V. A. Maroni
J. S. Patten, D. L. Smith, and C. K. Youngdahl

CTR Program
Argonne National Laboratory
Argonne, Illinois 60439

A primary energy conversion system designed for the ANL Tokamak Experimental Power Reactor consisting of, the first wall assembly, the blanket region, the magnet shield and the penetrations for plasma access are herein described.

INTRODUCTION

A scoping study[1] and a conceptual design[2] of a tokamak experimental power reactor (TEPR) have been completed. The design objectives of the TEPR are to operate for 10 years at or near electrical power breakeven conditions with a duty factor $\geq$ 50% and to demonstrate the feasibility of tokamak fusion power reactor technologies. A primary energy conversion system (PECS), capable of meeting these objectives, is herein described. The PECS consists of: (Figure 1 and 2), the first wall assembly; the blanket region (a 28-cm zone immediately backing the first wall); the primary coolant; the magnet shield; and the penetrations which provide access for the vacuum system, neutral beam injection, diagnostics, and experimental facilities.

Major efforts have been undertaken at ANL[1,2] and elsewhere[3,4] to define the objectives of a Tokamak Experimental Power Reactor (TEPR). The ultimate goal of these studies has been to establish the scientific and engineering basis for a detailed reactor design. This paper will concentrate on the TEPR primary energy conversion system (PECS) as developed in the ANL study. The PECS is considered to include all components that lie between the plasma and the toroidal field coils, e.g., the first wall, blanket, magnet shield, coolant, penetrations for vacuum interfacing, neutral injection beam lines, diagnostics, and maintenance access. Previous reports[1,5] have described the underlying philosophy used in developing design criteria for a PECS that would meet the needs of a TEPR. Reference 2 contains a detailed description for the PECS design that has evolved in the ANL/TEPR studies. This paper contains a summary of the details relating to both the PECS first wall and blanket/shield designs. Figures 1 and 2 show, respectively, the vertical section and plan view of the ANL/TEPR and give some perspective as to the location and configuration of PECS components. Features of many of the systems interfacing with the PECS are described in other papers presented at this meeting.[6-10]

* Work supported by the U.S. Energy Research and Development Administration.

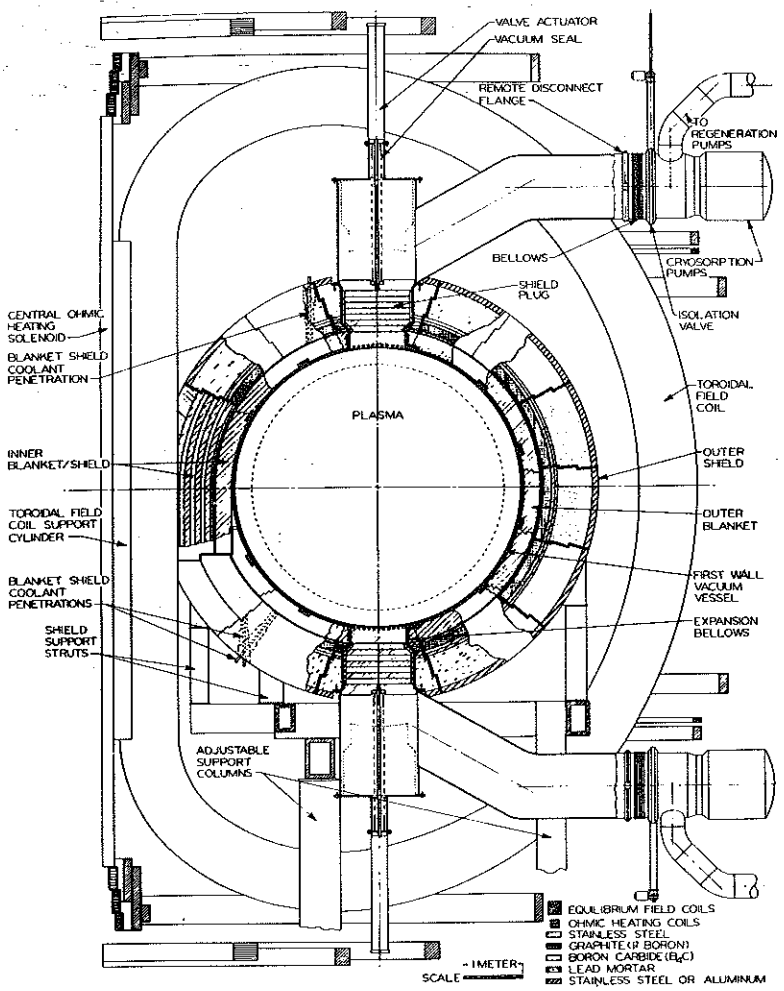

FIGURE 1. Vertical Section of EPR

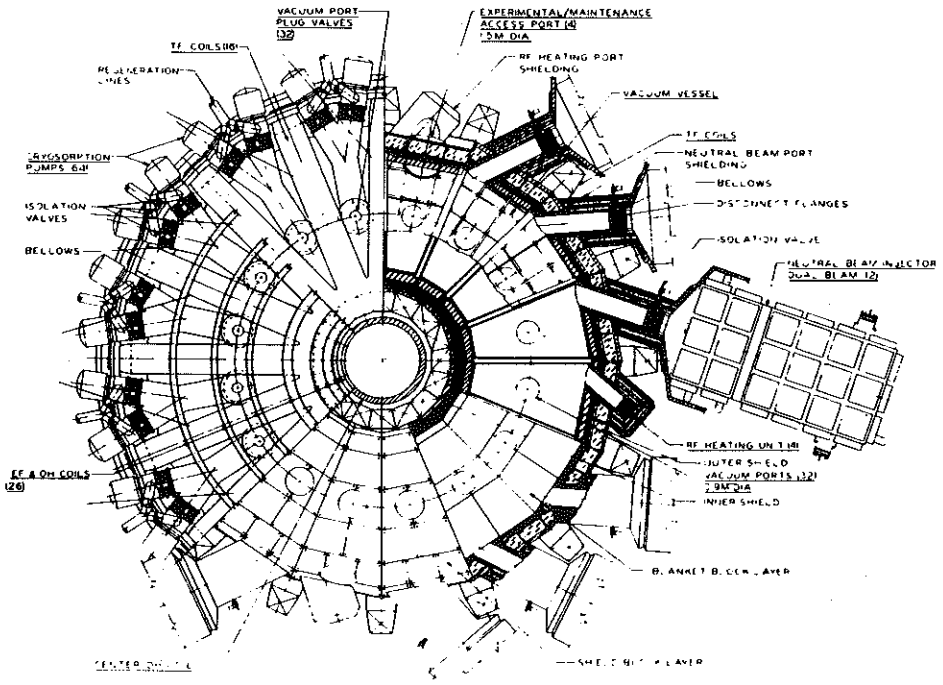

FIGURE 2. EPR Plan View

FIRST WALL

The first wall system (see Fig. 3) consists of a vacuum wall and detachable coolant panels. The free-standing vacuum vessel is constructed from 16 cylindrical segments of 2-cm thick stainless steel plate and is reinforced with an external ring and spar framework. Locations of the two circumferential support rings and ten longitudinal spars on each segment are shown in Fig. 3. The 16 segments are joined by formed rings that are welded to the ends of each segment. A chemically bonded Cr_2O_3 coating is applied to the joining surfaces in two of these rings to form a current breaker in the vacuum wall. The vacuum vessel wall is cooled by a separated pressurized water loop utilizing an integral nondetachable panel wall system as illustrated in Figure 3.

The surface of the detachable coolant panels facing the plasma is coated with 100-200 microns of beryllium to control impurity contamination of the plasma by stainless steel. The substantial porosity (10-15%) and fine microstructure obtainable with the plasma spray-coating process facilitates gas re-emission, particularly helium, and minimizes blistering erosion.

Water is supplied to these coolant panels by manifolds located in the connecting rings that join the first-wall segments. The toroidal vacuum wall is supported by a three-point per segment, roller/slide pad-type support from the blanket to the lower rings and spars. The three-point support minimizes the size of the reinforcing ring and the roller/slide support minimizes thermal stresses by allowing for

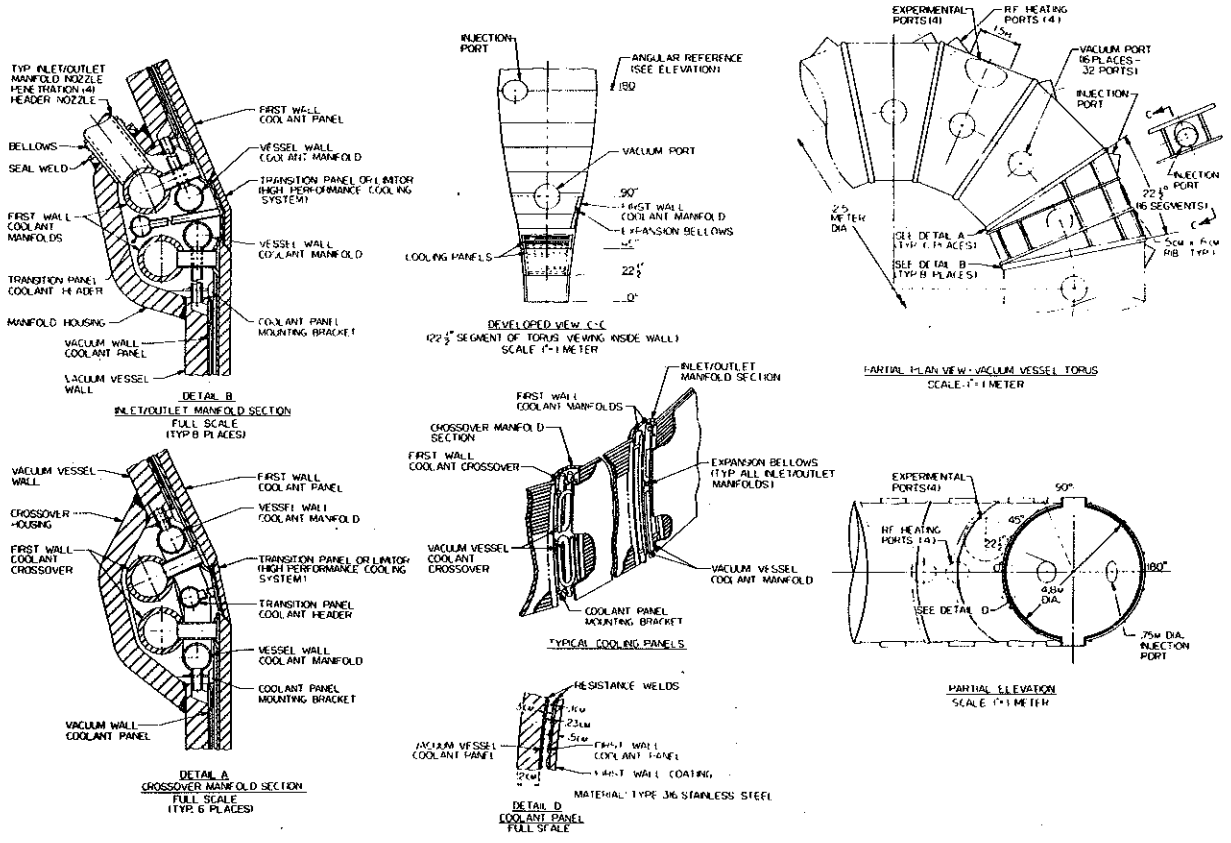

FIGURE 3. First Wall Vacuum Vessel Assembly

expansion of the vessel. The first wall design parameters are summarized in Table 1.

Extensive thermal-hydraulic, mechanical, materials response and radiation damage analyses have been performed to evaluate the first wall performance and to determine the design limits. Results are summarized in Table 2. The stainless steel vacuum wall should maintain its structural integrity for the 10 year design life under the nominal operating conditions, viz., integrated wall loading of 2.5 MW-yr/m^2, maximum annual neutron fluence of 6 x 10^{25} n/m^2 (2.8 dpa/year, 54 appm/year helium and 133 appm/year hydrogen) and maximum wall temperature of $\leq 500^{o}C$. For these conditions the predicted radiation swelling of < 4% is tolerable. The limiting criterion is loss of ductility caused by displacement damage and helium generation. For temperatures below $500^{o}C$, the residual uniform elongation, which is estimated to be $\geq$ 1% at the end of the 10 year life, is considered to be acceptable. The lifetime of the low-Z coating is limited by erosion caused primarily by D-T physical sputtering. A design life of 5 years for a 100 to 200-μm thick beryllium coating appears feasible. Only limited data exist with which to estimate the lifetime of the ceramic current breaker; however, bulk radiation effects will likely be the limiting criteria.

In addition to the extensive radiation damage, the coolant panel will be subjected to severe thermal cycling produced by heat deposition on the surface during the plasma burn. Temperature variations in the hottest coolant panel during operation are shown in Figure 4. The spike is caused by the radiation emitted when argon is injected to terminate the burn. The strain range for the burn cycle depends on the difference between the maximum and minimum values of ΔT during the cycle, and the strain range for the plant warm-up/cool-down operating cycle is a function of the average ΔT during the burn cycle. Assuming that the duration of the operating cycle is long enough that stress relief occurs, the strain range for the coolant panels with sliding supports is 0.085% for the burn cycle and 0.14% for the warm-up/cool-down operating cycle. These values correspond to fatigue design lifetimes for the coolant panels of 5 x 10^6 burn cycles and 1 x 10^5 operating cycles. Thus, thermal fatigue will limit the life of the coolant panel to 5 years, which corresponds to $\sim 10^6$ burn cycles, for the current design parameters.

Although the current first-wall system design is based to a large extent on available materials and existing technology, it appears that adequate mechanical integrity of the system can be maintained for suitable reactor lifetimes under the postulated EPR conditions.

BLANKET/SHIELD SYSTEM

The blanket/shield system consists of the blanket, the inner bulk shield, the outer bulk shield and the penetration shields. In order to insure penetration of the equilibrium field into the plasma region without intolerable distortion or phase delay, the blanket and bulk shield are constructed of 688 electrically insulated blocks, as illustrated in Fig. 5.

The blanket is made up of 0.28-m thick stainless steel blocks, as shown in Fig. 6. Each of the 16 segments of the vacuum chamber is covered by 17 blanket blocks. The blocks are cooled with pressurized water flowing in a network of 1-cm diameter drilled channels, with each block having an independent cooling system.

TABLE 1. First-Wall Design Parameters

Design Description

- Free-standing, stainless steel vacuum wall with rib and spar reinforcing.
- Detachable, water-cooled stainless steel panels to shield vacuum wall from plasma.
- Low-Z coating on plasma-exposed face of coolant panel for high-Z impurity control.

Design Parameters

Vacuum chamber	
Material	316 SS
Design stress (ksi)	10
Major radius (m)	6.25
Minor radius (m)	2.4
Volume (m^3)	711
Wall area (m^2)	592
Wall thickness (cm)	2
Ring and spar (cm)	
Width	5
Depth	11
Ports	
Vacuum (0.95 m diameter)	32
Heating (0.75 m diameter)	16
Experimental (1.5 m diameter)	4
Total port area (m^2)	31
Current breaker	
Material	Cr_2O_3
Form	Coating
Preparation	Chemical bond
Coolant panel	
Material	316 SS
Number	352
Area per panel (m^2)	1-2
Length (m)	1-2
Width (m)	$\sim$ 1
Total panel thickness (cm)	$\sim$ 1
Thickness front wall (cm)	0.5
Low-Z coating	
Material	Beryllium
Thickness (μm)	100-200
Preparation	Plasma spray
Coolant	H_2O

TABLE 2. First-Wall Operating Parameters and Design Limits*

Nominal Operating Conditions	
Capacity factor (%)	50
Operating cycle (s)	
Startup	5
Burn	35
Shutdown	5
Exhaust and replenishment	15
Average power loading during burn (MW/m^2)	
Neutron	0.5
Radiation, conduction, convection	0.13
Operating Parameters	
Stainless steel vacuum wall	
Maximum temperature (^oC)	< 500
Minimum yield stress at 500^oC (ksi)	17
Maximum annual fluence (n/m^2)	6×10^{25}
Neutron damage (dpa/yr)	2.8
Helium generation (appm/yr)	54
Hydrogen generation (appm/yr)	133
Stainless steel coolant panel	
Maximum temperature (^oC)	380
Minimum yield stress at 500^oC (ksi)	17
Maximum annual fluence (n/m^2)	6×10^{25}
Neutron damage (dpa/yr)	2.8
Helium generation (appm/yr)	54
Hydrogen generation (appm/yr)	133
Maximum heat deposition (W/cm^3)	5.5
Maximum ΔT across panel surface (^oC)	20
Maximum ΔT through panel face (^oC)	
With Argon shutdown	100
Without Argon shutdown	75
Maximum ΔT during burn cycle (^oC)	100
Maximum thermal strain range (%)	
Operating cycle	0.14
Burn cycle	0.09
Beryllium coating	
Maximum surface temperature (^oC)	407
Helium generation (appm/yr)	780
Hydrogen generation (appm/yr)	13
Maximum erosion rate ($\mu m/yr$)	30
Water coolant	
Maximum pressure (psi)	2000
Velocity (m/s)	1.6
Inlet temperature -- first panel (^oC)	40
Exit temperature -- eighth panel (^oC)	310
Pumping power (MW)	< 1
Vacuum wall	
Design life (yr)	10
Integrated neutron wall loading ($MW-yr/m^2$)	2.5
Yield strength -- 10 yr (ksi)	75
Uniform elongation -- 10 yr (%)	> 1
Radiation swelling -- 10 yr (%)	< 4
Limiting criterion	Ductility
Coolant panel	
Design life (yr)	5
Total burn cycles -- 5 yr	10^6
Fatigue lifetime (yr)	5
Radiation lifetime (yr)	8
Limiting criterion	Thermal fatigue
Low-Z coating	
Design life (yr)	3-5
Limiting criterion	D-T sputtering

* Based on a neutron wall load of 0.5 MW/m^2 and a plant capacity factor of 50%.

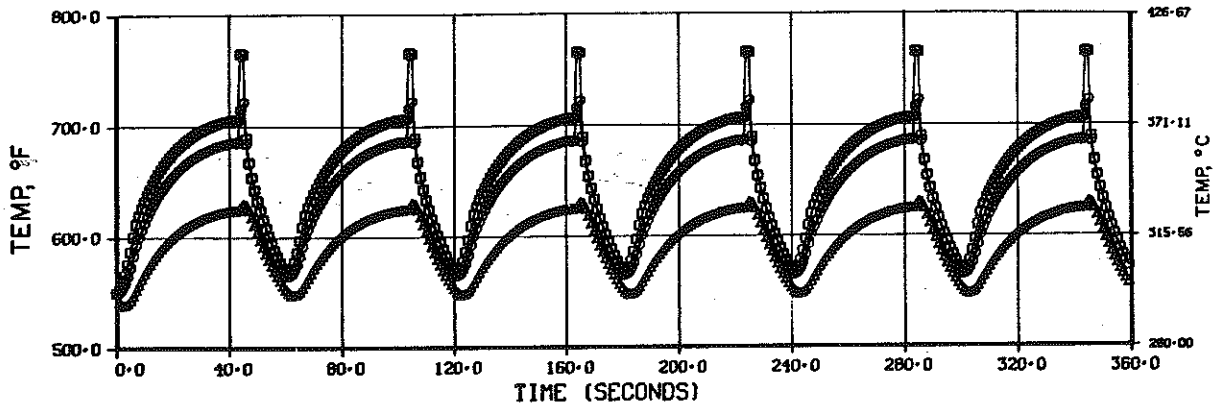

FIGURE 4. Transient Temperature Histories (0.5 MW/m^2) Locations on the Coolant Exit Plane at the Surface of the Beryllium Coating (upper curve), at the Surface of the Stainless Steel in Contact with the Coating (middle curve) and at the Stainless Steel Surface in Contact with the Coolant.

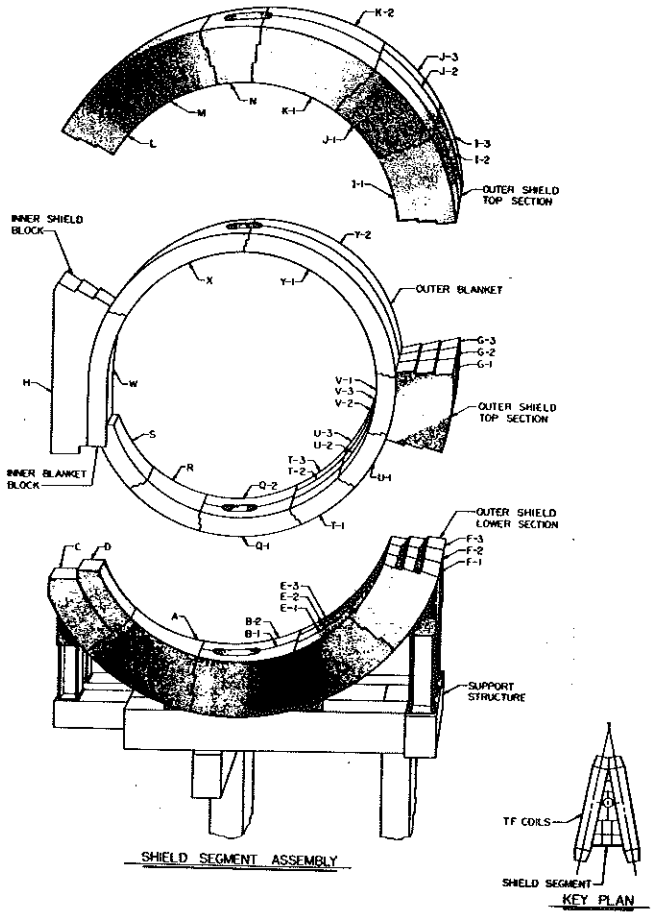

FIGURE 5. EPR Blanket/Shield Arrangement

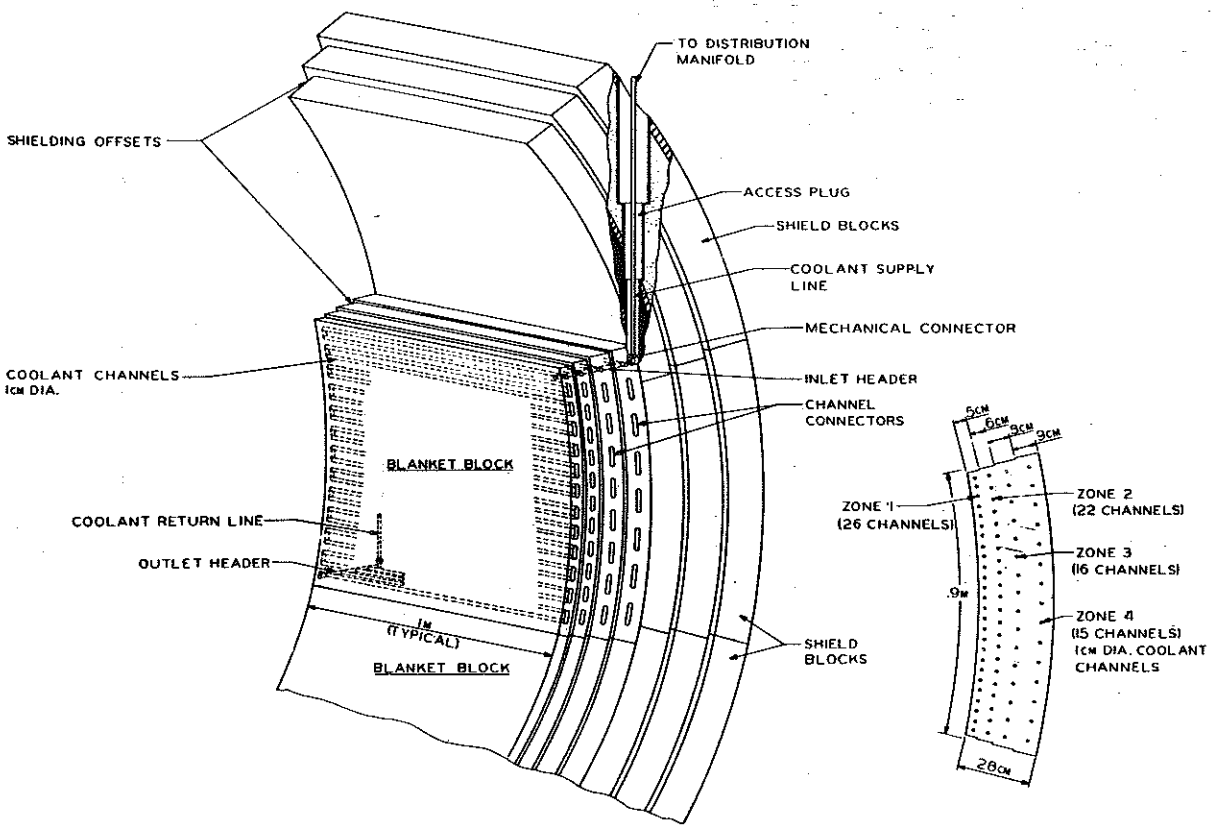

FIGURE 6. Blanket Block

The bulk shield surrounding each of the 16 segments of the vacuum wall and blanket consists of 1 inner shield block and 25 outer shield blocks, as shown in Fig. 5. The inner shield block is 0.58-m thick made up of alternating layers of B_4C and stainless steel disposed so as to maximize the attenuation of neutrons and gamma rays. At the top, bottom and outside of the torus, the bulk shield is 0.97-m thick and consists (going radially outward) of 0.03 m of stainless steel, 0.15 m of graphite with 1% natural boron, 0.05 m of stainless steel, 0.65 m of lead mortar and 0.09 m of aluminum. The bulk shield is cooled with H_2O at near atmospheric pressure.

Neutral beam lines, vacuum ducts and other penetrations of the outer blanket and bulk shield represent large ($\sim$ 0.6 to 1.0 m^2 cross section) streaming paths for neutrons and require special shielding. A special, 0.75-m thick annular shield surrounds the neutral beam tube after it exits from the bulk shield and extends beyond the TF coils, so that there is no unshielded line-of-sight path from the wall of the beam tube to the TF coils. The inner 0.65 m of this special shield is 50% SS/50% B_4C, followed by 0.05 m of lead and 0.05 m of aluminum.

A pneumatically operated shield plug is closed in the vacuum duct during plasma burn (see Fig. 1). This shield plug consists of two blocks. The inner block is 0.32-m thick and is fabricated of stainless steel and cooled in the same manner as a blanket block. The outer block is 0.58-m thick with a material disposition (SS/B_4C) similar to that of the inner shield.

The blanket, shield and vacuum vessel assembly weighs over 2700 metric tons. This weight is supported from beneath the

reactor on 16 individual frames. The frames can move vertically approximately two meters to facilitate replacement of the blanket and shield blocks. The load is transferred through 32 columns from the reactor foundation to the 16 frames, which in turn support the reactor shielding blocks. The blanket block layer rests on the inner portions of the shield blocks on insulation roller pads to accommodate the high temperature of the blanket and the accompanying thermal expansion. The 350 metric ton vacuum vessel rests on the inner side of the lower blanket blocks.

Extensive analyses have been performed to evaluate the performance of the blanket/shield system. These analyses are based on a nominal neutral wall load of 0.5 MW/m^2 and a plant capacity factor of 50%. Results are summarized in Tables 3 and 4. Radial distributions of the neutron heating rate and of the atomic displacement are shown in Figs. 7 and 8.

The 4-cm first wall and the 28-cm blanket region receive $\gtrsim$ 90% of the gamma energy. For the most part, the properties and requirements of the blanket material are the same as those of the first wall. The radiation damage level adjacent to the first wall is $\sim$ 1.7 dpa/year and drops by a factor of two every $\sim$ 7 cm going through the blanket. Operating temperatures in the load bearing portions of the blanket are, like the first wall temperatures, restricted to $\leq 500^{o}C$, but may be allowed to rise above this level in non-structural components. In general, the less severe radiation environment of the blanket will mean that property changes will be less than in the first wall. After 10 years at a wall loading of 0.5 MW/m^2 and a 50% capacity factor, the swelling in the blanket adjacent to the first wall is expected to remain below 2%, the uniform elongation will drop to $\sim$ 3%, and the yield strength will increase to $\sim$ 75 ksi. As the neutron radiation is attenuated through the blanket, the swelling will be reduced to zero after a few cm, and the tensile properties will approach those of unirradiated material ($\sim$ 22% uniform elongation and $\sim$ 17 ksi yield strength). The effect of creep and fatigue will be less than in the first wall since the blanket is not exposed to the surface radiation from the plasma and will not undergo the large thermal cycling of the first wall. Helium production rates will still be high in the first few cm, but the temperature limit of $500^{o}C$ should reduce the possibility of helium embrittlement, which is observed at temperatures above $550^{o}C$.

The bulk shield will receive < 5% of the total radiation energy produced in the EPR. No degradation of the bulk properties of stainless steel is expected. The boron carbide located in the inner shield is a brittle material with moderate tensile strength and high compressive strength. The major effect of radiation on boron carbide is the buildup of helium from (n,α) reactions that can induce swelling and cracking if it is present in high concentrations. Neutron irradiation can also substantially reduce the thermal and electrical conductivity. The degree to which radiation affects the bulk properties depends to a large extent on the amount of porosity present in the unirradiated material. The first layer of boron carbide in the inner shield will be the most seriously affected by the neutron irradiation. The first few cm of boron carbide will produce $\sim$ 3500 appm of helium

TABLE 3. Summary of Blanket Design Parameters

Design basis operating life (yr)	10
Nominal power during burn (MW)	400
Design basis neutron wall loading (MW/m^2)	0.5
Plant capacity factor (%)	50
Blanket structure	
Thickness (m)	0.28
Type metal/volume fraction	316-SS/0.9
Type coolant/volume fraction	$H_2O/\leq 0.05$
Penetration volume fraction	
Inner blanket	$\sim$ 0.02
Outer blanket	$\sim$ 0.05
Maximum temperatures (^oC)	
In support structures	500
In bulk materials	550
Nuclear parameters	
Maximum heat deposition (W/cm^3)	3.5
Maximum fluence at 2.5 MW-yr/m^2 (n/m^2)	5×10^{26}
Maximum dpa at 2.5 MW-yr/m^2 (dpa)	17
Maximum helium production at 2.5/MW-yr/m^2 (appm)	230
Maximum hydrogen production 2.5/MW-yr/m^2 (appm)	600
Mechanical parameters	
Design stress in support structure (ksi)	$\leq$ 10
Minimum material yield stress (ksi)	20
Ductility at 2.5 MW-yr/m^2 (% uniform elongation)	$\geq$ 3
Swelling at 2.5 MW-yr/m^2 (% of initial volume)	$\leq$ 2
Maximum torque from pulsed fields (ft-lb)	125,000
Coolant parameters	
Type	H_2O
Maximum pressure (psig)	2000
Pressure drop (psig)	< 15
Maximum velocity (m/s)	2.4
Pumping power (MW)	< 1
Coolant inlet temperature (^oC)	40
Maximum coolant exit temperature (^oC)	309
Residual activity from blanket/shield radiation waste after 2 yr operation (Ci/MWt)	
Immediately after shutdown	3.5×10^6
1 yr after removal	8.0×10^5
10 yr after removal	7.0×10^4
100 yr after removal	60

TABLE 4. Summary of Shield Design Parameters

Design basis operating life (yr)	10
Shield structure	
Thickness (m)	
Inner bulk shield	0.58
Outer bulk shield	0.97
Beam duct shield	0.75
Evacuation duct shield (movable plug)	0.90
Biological shield	1.5
Materials	
Inner shield	304-SS/B_4C
Outer shield	304-SS/Pb mortar/C/Al
Beam duct shield	304-SS/B_4C/Pb/Al
Evacuation duct shield (movable plug)	304-SS/B_4C
Biological shield	Concrete
Temperature (^oC)	$\leq 100^oC$
Coolant	H_2O
Maximum torque from pulsed fields (ft-lb)	253,000
Maximum nuclear heating in bulk shield (W/cm^3)	0.3
Fraction of fusion power deposited in shield	< 0.05
Maximum energy current at outer surface of bulk shield (W/cm^2)	
Neutrons	$\sim 2 \times 10^{-4}$
Gammas	$\sim 5 \times 10^{-5}$

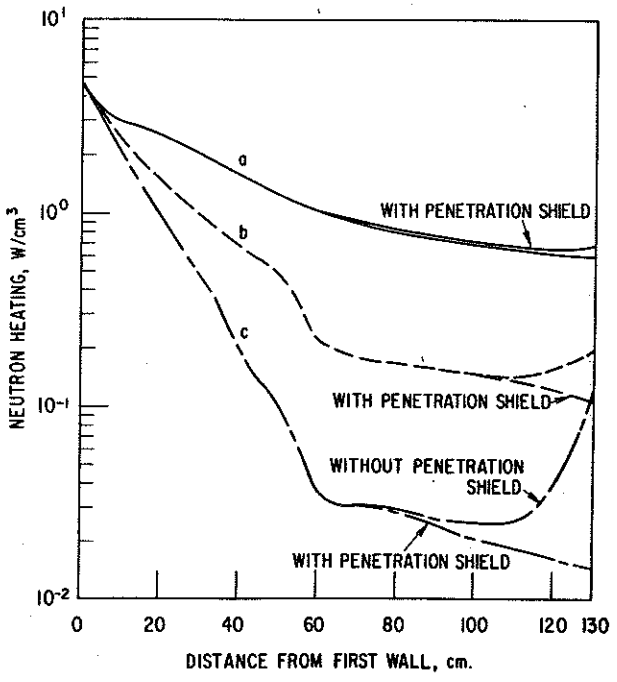

FIGURE 7. Neutron Heating in the Water Coolant as a Function of Depth in the Blanket/Shield for Three Locations with Respect to the Neutral Beam Duct: (a) at the wall of the beam duct, (b) at 10 cm from the wall of the beam duct and (c) at 30 cm from the wall of the beam duct.

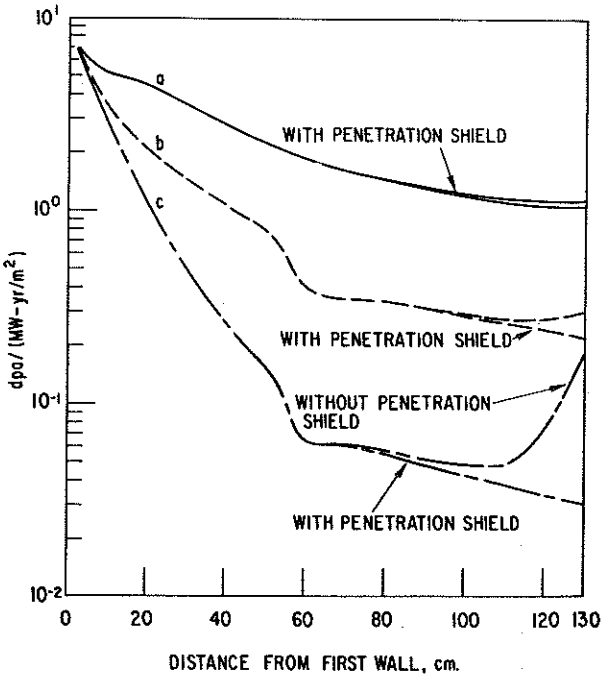

FIGURE 8. Atomic Displacement in Stainless Steel as a Function of Depth in the Blanket/Shield for Three Locations with Respect to the Neutral Beam Duct: (a) at the wall of the beam duct, (b) at 10 cm from the wall of the beam duct and (c) at 30 cm from the wall of the beam duct.

during a 10 year lifetime, but helium production will fall off rapidly past this point. This amount of helium is not expected to induce significant swelling or cracking if a sufficient porosity exists to accommodate the gas. Helium escaping from the boron carbide must be vented to prevent buildup of gas pressure within the shield. For the conditions expected in the EPR, the graphite in the outer bulk shield will densify rather than swell. It is expected that the volume change of graphite due to irradiation can be minimized by a suitable choice of material and should not present a problem. Helium production in the first few cm of the graphite with 1% boron will reach $\sim$ 770 appm after a 10 year lifetime. As with boron carbide, porosity and venting considerations must be factored into the shield design to accommodate the helium. The materials lying past the first layer of boron carbide in the inner shield and the graphite in the outer shield receive a relatively small neutron fluence, and the bulk properties should not be adversely affected. The lead mortar and aluminum in the outer shield will operate at temperatures below 100°C, which is well below the $\sim$ 150°C at which the lead mortar will begin to break down.

The radioactive inventory as a function of time for the EPR is shown in Figure 9. The level of neutron induced activation after two years operation is 3.5 x 10^6 Ci/MWt and decreases by a factor of 4 one year after shutdown and more rapidly for longer times. The curies per thermal megawatt are fairly independent of neutron wall loading for the range of 0.1 to 5 MW/m^2.

At shutdown, the decay heat is 2.5% of operating power and only drops about 20% during the first few minutes after shutdown,

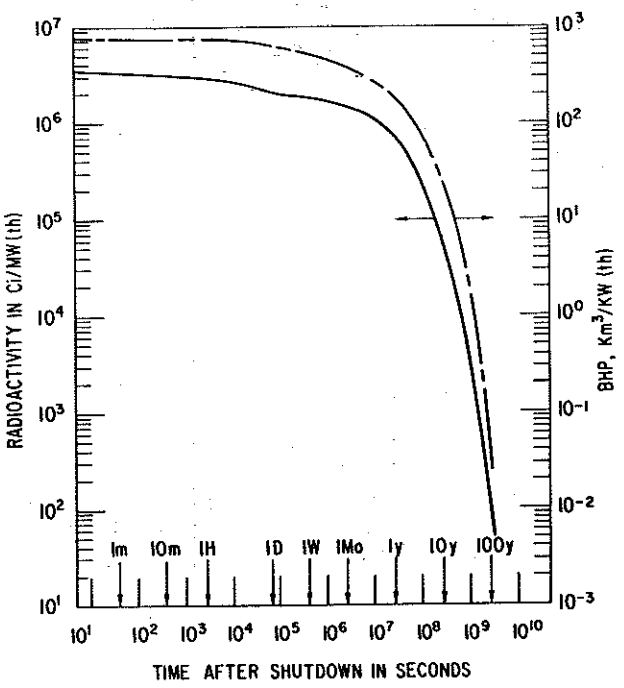

FIGURE 9. Radioactivity and Biological Hazard Potential as a Function of Time after Shutdown Following Two Years of Operation.

which is the period of time that is very crucial to emergency cooling.

During operation, the biological dose in regions external to the TF coils is about 10^6 mrem/hr, which is too high to permit access to the inside of the reactor building for any reasonable length of time. Outside the 1.5-m thick concrete building wall, the dose is about 1 mrem/hr. The biological dose in the vacuum chamber inside the first wall is 6 x 10^9 mrem/hr at shutdown and after one year of cooldown the dose is 1 x 10^9 mrem/hr. After one day of cooling, the dose is 600 mrem/hr at a position above the reactor at the location of the TF coils and 2 mrem/hr outside the TF coils. The latter result does not include the effect of penetration streaming or activation of the neutral beam injector. These calculations indicate that for a long period after shutdown the dose rate is too high to permit unshielded personnel access to the reactor building (in the region exterior to the TF coils) unless all pene-

trations and beam injectors are fully shielded.

The general approach to maintenance for the EPR is by use of remote handling apparatus. All large components will be repaired in place, where possible. This includes the vacuum vessel and the lower EF and OH coils. Smaller components like the blanket and shield blocks will be repaired in the hot cells. Special in-vessel remotely operated equipment will be designed to repair, replace and inspect any portions of the vacuum vessel or first-wall panels that have been damaged. Support facilities for remote operations include a remotely-operated overhead crane/manipulator with a shielded personnel cab, floor-mounted snorkel type units for servicing the vertical portions of the reactor and basement-positioned apparatus for maintaining the lower components of the reactor. A full-scale, quarter section mockup of the reactor is vital to all remote operations because it will be used to program the repair apparatus and perform practice runs.

REFERENCES

1. W. M. Stacey, Jr., et al., "Tokamak Experimental Power Reactor Studies," ANL/CTR-75-2, Argonne National Laboratory (June, 1975).
2. W. M. Stacey, Jr., et al., "Tokamak Experimental Power Reactor Conceptual Design," ANL/CTR-76-3, Argonne National Laboratory (August, 1976).
3. M. Roberts, et al., "Oak Ridge Tokamak Experimental Power Reactor Study - Reference Design," Oak Ridge National Laboratory (August, 1976).
4. C. C. Baker, et al., "Experimental Power Reactor Conceptual Design Study," GA-A-13534, General Atomic Co., (July, 1975).
5. J. S. Patten, et al., "A Primary Energy Conversion System for the Tokamak Experimental Power Reactor," Proceedings of the Sixth IEEE Symposium on Engineering Problems of Fusion Research, San Diego, California, November 16-21, 1975.
6. W. M. Stacey, Jr., et al., "Tokamak Experimental Power Reactor," Proceedings of the Second ANS Topical Meeting on the Technology of Controlled Nuclear Fusion, Richland, Washington, September 21-23, 1976.
7. M. A. Abdou, et al., "Multidimensional Neutronics Analysis of Major Penetrations in Tokamaks," ibid.
8. W. M. Stacey, Jr., et al., "Impurity Control in Near-Term Tokamak Reactors," ibid.
9. S. T. Wang, et al., "Conceptual Design of Superconducting Magnet Systems for the Argonne Tokamak Experimental Power Reactor," ibid.
10. F. E. Mills, et al., "Plasma Driving Systems for a Tokamak Experimental Power Reactor," ibid.